PCCP

Accepted Manuscript

ROYAL SOCIETY OF CHEMISTRY

www.rsc.org/pccp

Journal Name

ARTICLE

Playing with isomerism and N substitution in pentalenedione derivatives for organic electrode batteries: how high are the stakes?

Received 00th January 20xx,
Accepted 00th January 20xx

DOI: 10.1039/x0xx00000x

www.rsc.org/

Daniele Tomerini,[ab] Carlo Gatti[c] and Christine Frayret[ab*]

New concepts to design innovating and top-performing redox-active organic molecules based electrodes should push forward and promote an eco-friendly alternative to classical Li-ion batteries. In this promising research area, density functional theory calculations lend support to experiment through the prediction of redox voltage and give the promise to rationalize the trends, thus providing a general approach for engineering advanced materials. In this study in which we analysed spin density distribution along with Bader's partitioning of the molecular space and energies, a vision for designing pentalenedione derivatives with fine tuning of the redox potential properties is presented. The concept relies on joined effects of isomerism and N single/double substitution for C on the parent backbone. Such dual nature modification is able to provide a series of compounds within the range of 2.2 – 3.6 V *vs.* Li$^+$/Li (against a more restricted range of 2.2 – 2.8 V *vs.* Li+/Li for the sole effect of isomerism on the unsubstituted parent compounds). The incidence of double N substitution alone follows an almost additive rule based on the combined actions of the composing single N substitutions. Few exceptions to the rule were, however, also observed and rationalized. Beyond learning gained for this peculiar family, these results may have exciting implications for future design strategies.

Introduction

Organic electrode materials started to gain considerable attention in the last decades as they can originate from environmentally friendly and abundant resources (biomass) and since they at least improve a lot the cycle life of batteries (with much reduced cost and greenhouse gas emission). The possibility of fabricating lightweight and flexible devices by calling to such electrodes also corresponds to valuable merits. The synthetic versatility and modularity to tune electrochemical properties along with their ease in recycling after their lifetime as well as the possible involvement of multi-electron reactions are further conspicuous advantages of this class of materials. Many organic redox active families were already identified, including compounds incorporating carbonyl groups (see *e.g.* [1-9]), carboxylates (see *e.g.* [10-14]), polymeric Schiff bases (–N═CH–Ar–HC═N–)[15], ... However, lack of knowledge in terms of structure-property relationships or QSAR (Quantitative Structure Activity Relationship) may prevent defining guidelines for an effective selection of the most promising electrode candidates. This limitation may in turn leads to hampering progress in advancing organic battery technology.

Experimental trial and error tests based on potentially ideal combination of backbone, redox centre and functionalization, according to voltage properties already measured in other synthesized compounds, are key to the approach of searching for novel electrochemical functional materials. For instance, isomerism was recognized to play a role in the voltage (see *e.g.* [16]). On the other hand, while it has been proved recently that substituting N for C in anthraquinone may be beneficial for the voltage increase [17], there is no extended screening or established rule that may be used to clearly anticipate the effect of such structure manipulation in any kind of materials. Although some relationship between redox voltage and global molecular indicators such as electrophilicity, LUMO energy levels,… (see *e.g.* [18,19]) have been already established from theoretical studies, we are still far from the degree of understanding and knowledge regarding structure-redox activity that may pave the way towards advertised selection prior to experimental characterization.

In particular, one of the main difficulties lies in the fact that various contributions of the diverse constituents of a molecule cannot be disentangled when dealing solely with *global* molecular indicators. Thereby, the incidence in terms of redox voltage for the combination of one particular backbone with certain redox centres or for the relative positioning of one particular type of redox centre with respect to functional

---

[a] *Laboratoire de Réactivité et Chimie des Solides, UMR CNRS 7314, Université de Picardie Jules Verne, 33, Rue Saint-Leu, 80039 Amiens, France.*
[b] *Réseau sur le Stockage Electrochimique de l'Energie (RS2E), FR CNRS 3459, France*
[c] *CNR-ISTM, Istituto di Scienze e Tecnologie Molecolari, via Golgi 19, 20133, Milano, Italy.*

Electronic supplementary information (ESI) are available. Computational details; redox potential and free energy values, geometrical features, electron and electron spin populations for O and N, spin density patterns. See DOI: 10.1039/x0xx00000x groups are difficult to anticipate since they cannot simply correspond to values that are transposable from one compound to another. One further strategy to address the challenge of optimized materials discovery or at least to accelerate such process may correspond to an educated guess of mechanisms and rules governing the magnitude of redox voltage gained through accurate analysis of suitable *local* indicators or decomposition of *global* indicators into their constitutive components. This is where computational modelling can in particular take part into the game of identifying the most promising candidates. By collecting redox voltages and accurately dissecting this property into the contributions coming from each part of the molecule(s), one should be able to provide some consistent and extended selection criteria, provided that a common methodology can be identified to work on various classes of compounds. As a contribution to this ultimate goal, we present here a simulation study restricted to the family of the pentalenediones in which the effect of both isomerism and substitution of N for C (leading for instance to Pyrrolo[3,4-c] pyrrole-1,4-dione, or PPD) were probed. This work follows another investigation, whereby we were able to provide a deep insight into the mechanisms underlying the division of quinoneazine derivatives (quinoid-like structures separated through a bridge) into low- and high-voltage systems according to the indirect incidence of the bridge chemical bonding nature [20]. Such an understanding was reached by examining how the structural, electronic and energetic properties of quinoneazine derivatives evolve from their initial (neutral and unreduced) to their final (charged radical and reduced) forms and by using both global and local energy/bonding indicators to shed light on such evolutions.

Computational methods

All the calculations were conducted using Gaussian09 quantum chemistry package of programs [21]. The geometry of each species was fully optimized using the B3LYP/6-31+G(d,p) method. Each optimized structure was checked by frequency calculations to be a real minimum without any imaginary frequency at the same level of theory used in the geometry optimization. The free energy was evaluated using ZPE, thermal corrections (0-298 K) and the entropy term. The calculations of gas phase free energies use a reference state of 1 atm and 298 K. Solvation energies were estimated with the SMD approach [22] that was found to give an improved description of solvation energies compared to other several popular implicit solvent models such as COSMO-RS, IEF-PCM, C-PCM [23] and was already selected in the literature for the study of carbonyl-based organic compounds (see *e.g.* [20,24,25]). The absolute standard redox potential values for the one-electron reduction process, $E^0_{red\,(solv)}$ were extracted from the evaluation of the Gibbs free energy difference characterizing the initial, neutral pentalenedione (P) and the corresponding 1-electron reduced, radical ion ($P^{-\bullet}$), $\Delta G^0_{red\,(solv)}$according to the Nernst Equation (1):

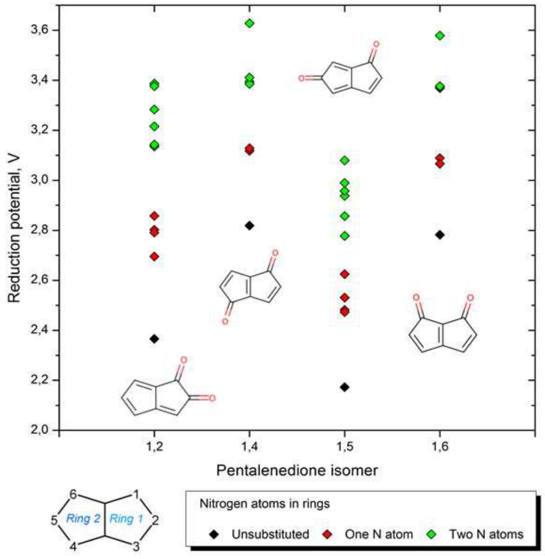

Fig. 1 Reduction potentials (in V vs. Li+/Li) for the parent pentalenediones and all their singly and doubly N-substituted derivatives. Numbering used for the atom position identification and ring nomenclature are reported.

$$E^0_{red\,(solv)} = \frac{-\left(\Delta G^0_{red(solv)}\right)}{nF} \qquad (1)$$

where *n* is the number of electrons (here equal to 1) in the electron-transfer half reaction and F is the Faraday constant (see ESI for further details on the evaluation of $\Delta G^0_{red\,(solv)}$).

The value of 1.46 V proposed by Vollmer *et al.* [26] was used to get voltages relative to the Li^+/Li reference electrode, according to Equation (2):

$$E^0_{vs\ Li/Li^+} - E^0_{red\,(solv)} - 1.46\,V \qquad (2)$$

The partition of the molecular space into atomic basins was performed according to the Quantum Theory of Atoms in Molecules (QTAIM) [27]. Atomic electron and electron spin populations charges, spin densities and atomic energies were calculated through slightly modified versions of the Extreme and PROMEGA programs [28] and using the wavefunctions of the solvated systems. Further details and explanations regarding the reliability and approximations of our approach are provided in the ESI.

Results and discussion

In the present screening of pentalenediones, all possible carbonyl positions and all single or double CH replacements by N were considered. We labelled the N-substituted compounds as X,Y_N(A) or X,Y_N(A,B), where X and Y denote the carbonyl positions and A (or A,B) the position(s) of replaced CH group(s) for single and double substitutions (Figure 1). For instance, 1,2_N(3,4) corresponds to the 1,2 pentalenedione with N atoms replacing CH groups at positions 3 and 4, while 1,2_N(0,0) stands for the corresponding unsubstituted compound.

Reduction potentials for all investigated pentalenedione systems (lying within the range 2.2–3.6 V *vs.* Li^+/Li) are portrayed in Figure 1 and extensively reported in Table S1 of the ESI. Despite the molecular state character inherent to these investigations, which might involve a certain degree of – potentially not constant/systematic – shift with respect to the observed intercalation potentials of actual crystalline materials involved as electrodes, the interpretation of ranking in voltages of such entities might provide some clues to the experimentalists for a fast/cheap rough screening.

From data in Figure 1 one observes that reduction potential of the unsubstituted compounds depends upon the relative position of the two carbonyl groups, with 1,4_N(0,0) and 1,6_N(0,0) having the largest and almost equivalent potential value of about 2.8 V *vs.* Li^+/Li while the 1,2_N(0,0) and 1,5_N(0,0) exhibit voltages around 2.4 and 2.2 V *vs.* Li^+/Li respectively. The highest increase upon double N substitution is found for the 1,2 system for which more than 1.0 V is gained. Indeed, the replacement of one or two CH groups by N always increases the reduction potential and roughly by similar magnitudes for all parent compounds (about 0.3-0.4 V/0.8-1.0 V for single/double CH replacements). The potential value of N-substituted compounds is thus primarily determined by their parent compound potentials, though an important secondary effect due to the position(s) of CH group replacement is also visible.

To clarify such secondary effect we considered the free energy changes of both the initial (I) neutral and final reduced (R) forms upon CH replacement(s) by N atom(s). They are denoted as $\Delta G_{CH\rightarrow N}$(I) and $\Delta G_{CH\rightarrow N}$(R), respectively, and evaluated as the difference between the free energy value of the N-substituted compound and that of the corresponding parent compound. Note that all our investigated systems are characterized by $[\Delta G_{CH\rightarrow N}(R)]/[\Delta G_{CH\rightarrow N}(I)] > 1$, as N substitution was found to always comply with a reduction potential increase. Values of $\Delta G_{CH\rightarrow N}$(I) and $\Delta G_{CH\rightarrow N}$(R) for all singly and doubly substituted compounds are displayed in Figure S1 of the ESI as a function of the calculated potential, while Figure 2 portrays such values for two representative cases, the N-substituted compounds having 1,2_N(0,0) and those having 1,4_N(0,0) as parent molecules. The former set of compounds exhibits well differentiated reduction potential values, for both single and double N-substitution, while, in general, the latter shows a much smaller differentiation within each set of values. By focusing first on *single* N-substitution, Figure 2 shows that both the $\Delta G_{CH\rightarrow N}$(I) and $\Delta G_{CH\rightarrow N}$(R) values do not exhibit a monotonic trend with increasing potential in the case of the 1,2 derivatives.

This observation implies that their spread of potential values does not occur because of a regularly decreasing stabilization of their initial forms and (or) because of a corresponding increase of the stabilization of their reduced forms with increasing potential value. Rather, in the case of 1,2 derivatives, the energy of initial and reduced forms decreases in magnitude on passing from the 1,2_N(4) to the 1,2_N(5) system and then it is found to increase for systems that are N-substituted at the position (6) and particularly at the (3) one. The voltage trend from the lowest to the highest potential

Table 1: Singly/doubly N-substituted systems: Initial (I) and Reduced (R) forms free energy changes upon CH replacement(s) by Nitrogen(s), $\Delta G_{CH\rightarrow N}$ (I) and $\Delta G_{CH\rightarrow N}$ (R), respectively. Comparison between the values estimated through the sum of the singly N-substituted systems free energy changes (*i.e.* extracted from the additivity rule) (Σ_{AR}) and the difference between $\Delta G_{CH\rightarrow N}$ and Σ_{AR} (Δ) is also displayed.

System	$\Delta G_{CH\rightarrow N}(I)^a$	$\Sigma_{AR}{}^a$ *(Δ)*^{b}	$\Delta G_{CH\rightarrow N}(R)^a$	$\Sigma_{AR}{}^a$ *(Δ)*^{b}
1,2_N(4)	-16.050		-16.062	
1,2_N(5)	-16.041		-16.057	
1,2_N(6)	-16.043		-16.059	
1,2_N(3)	-16.046		-16.064	
1,2_N(4,6)	-32.097	-32.093 *(-0.004)*	-32.121	-32.121 *(-0.005)*
1,2_N(4,3)	-32.097	-32.096 *(-0.001)*	-32.126	-32.126 *(-0.002)*
1,2_N(4,5)	-32.059	-32.091 *(0.032)*	-32.119	-32.119 *(0.023)*
1,2_N(5,6)	-32.064	-32.084 *(0.020)*	-32.116	-32.116 *(0.023)*
1,2_N(5,3)	-32.083	-32.087 *(0.004)*	-32.121	-32.121 *(0.005)*
1,2_N(6,3)	-32.079	-32.089 *(0.010)*	-32.123	-32.123 *(0.006)*
1,4_N(2)	-16.058		-16.069	
1,4_N(3)	-16.041		-16.052	
1,4_N(2,5)	-32.111	-32.116 *(0.005)*	-32.132	-32.138 *(0.006)*
1,4_N(2,6)	-32.097	-32.099 *(0.002)*	-32.119	-32.121 *(0.002)*
1,4_N(2,3)	-32.062	-32.099 *(0.037)*	-32.091	-32.121 *(0.030)*
1,4_N(3,6)	-32.079	-32.082 *(0.003)*	-32.100	-32.104 *(0.004)*

a) All energies are in Hartree (Ha). *b*) A negative (positive) Δ value means stabilization (destabilization) relative to the prediction given by the additivity rule.

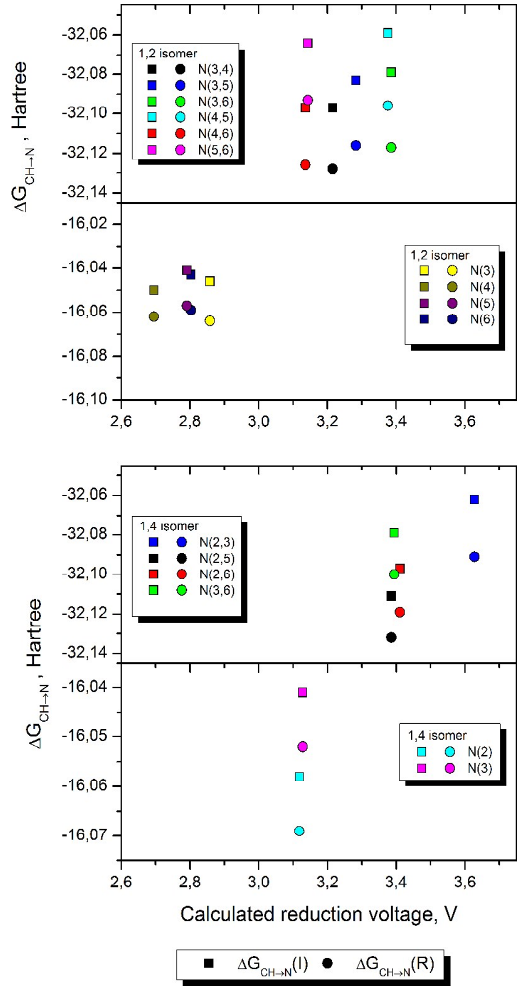

Fig. 2: Initial (I) and Reduced (R) forms free energy changes upon CH replacement(s) by Nitrogen(s) ($\Delta G_{CH\rightarrow N}$) for the singly and doubly N-substituted 1,2 (top) and 1,4 (bottom) pentalenedione derivatives.

system is solely the result of an increasing gain in stabilization upon reduction, while it does not imply any monotonic trend of their energies in either initial/reduced series with increasing potential, as it is often the case when a series of electron donating or electron withdrawing substituents are introduced on a given backbone. Such a behaviour is even more evident in the case of 1,4 derivatives. Here, just two quite chemically distinct positions, namely (2) and (3), may be N-substituted and this fact results in totally dissimilar energies for both their initial and reduced forms (note that the [1,4_N(2)] derivative is so stabilized relative to [1,4_N(3)] that its initial form has an energy comparable to that of the [1,4_N(3)] reduced form). However, since the relative stabilization of their reduced forms is very much alike, their potentials are almost indistinguishable.

Table 2: Reduction potentials (V) (in V *vs.* Li^+/Li) for the parent compounds, corresponding subsystem energies at the initial and reduced state for ring 1 (R1) plus ring 2 (R2) (E_I (R1+R2) and E_R (R1+R2)), respectively, and their changes from reduced to initial forms (ΔE(R1+R2)). Related changes for global oxygen atoms energies (ΔE(O)), and total energy variations for the whole molecule (ΔE_{TOT}) are also listed.

System	Voltage, V	E_I (R1+R2)^a	E_R (R1+R2)^a	ΔE(R1+R2)^a	ΔE(O)^a	$\Delta E_{TOT}{}^a$
1,5_N(0,0)	2.173	-305.800	-306.066	-0.265	+0.133	-0.132
1,2_N(0,0)	2.366	-305.797	-306.010	-0.212	+0.074	-0.138
1,6_N(0,0)	2.782	-305.782	-306.054	-0.272	+0.119	-0.153
1,4_N(0,0)	2.819	-305.760	-306.048	-0.288	+0.134	-0.155

a) All energies are in Hartree (Ha).

The situation becomes more complex when double CH replacements are considered. All possible and unique pair substitutions can now be exploited, giving rise, for instance, to 6 and 4 doubly-substituted derivatives for 1,2 and 1,4 parents, respectively. The resulting redox potential spreading for 1,2 derivatives is almost doubled (about 0.28 V) relative to single-substitution and the $\Delta G_{CH\rightarrow N}$ values of initial and reduced forms may in general be roughly predicted by summing up the values of the single-substitutions composing the pair. As a result, the changes in the redox potential values relative to that of the unsubstituted compound are approximately given by the sum of the voltage gains of the singly substituted compounds (see Table S1 and Figure 1). Notable exceptions are those doubly substituted systems where the two N are contiguous and linked to one another, like for the [1,2_N(4,5)] and [1,2_N(5,6)] compounds for which energy losses relative to the additivity rule are as large as 0.032 and 0.020 Ha / 0.023 and 0.023 Ha for the initial / reduced forms, respectively (see Table 1). This is a clear indication that the presence of two contiguous N is destabilizing for the systems. However, such destabilization affects differently the reduced and initial forms, being larger for the initial form in [1,2_N(4,5)] and larger for the reduced form in [1,2_N(5,6)]. Consequently, the corresponding redox potentials are respectively higher (1.01 V) and smaller (0.78 V *vs.* Li^+/Li) than their additivity rule estimates of 0.75 and 0.87 V *vs.* Li^+/Li. A chemical rationalization for such different behaviour can be found by considering the presence of a double N=N bond in the dominant resonance form of the initial structure of [1,2_N(4,5)], which is energetically unfavourable for the N (*see infra* the discussion on QTAIM energy analysis), while both the reduced resonance forms of this molecule and the two initial and reduced forms of [1,2_N(5,6)] are not characterized by

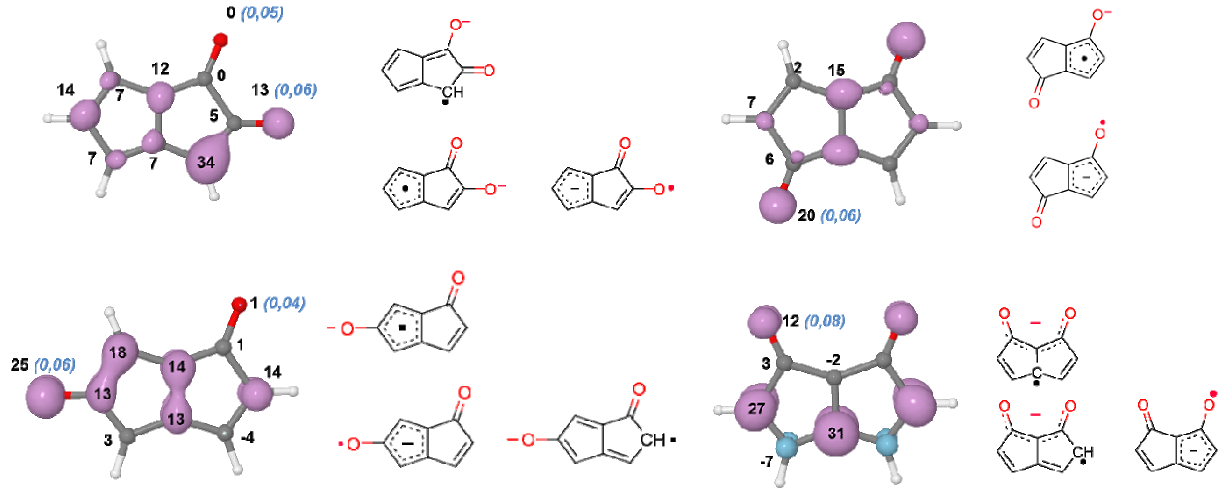

Figure 3: Spin density patterns and most relevant resonance forms for the reduced forms of the parent pentalenediones. An isocontour value of 0.0075 electron (magenta: positive; light blue: negative) was used to plot the spin density distribution isosurface. Bader's atomic spin density populations (in hundredths of an electron) are presented as well. O electron population increases upon reduction are also shown (values in blue/in parentheses).

such a bond feature, as evidenced as well through the bond distances analysis (see Table S2). Similar reasoning applies to the set of 1,4 doubly substituted compounds in which [1,4_N(2,3)] is the only one that markedly differs in the redox potential value relative to the other derivatives since it largely deviates from the additivity rule. Once again, this originates from the occurrence of two contiguous N in the compound and to the presence of a double N=N bond in the initial form. Given the similar potential values for the two singly N-substituted 1,4 derivatives and the strict adherence to the additivity rule for all 1,4 doubly substituted compounds other than [1,4_N(2,3)], these various systems exhibit an almost constant potential. Interpretation of redox voltages for singly and doubly N-substituted 1,5 and 1,6 compounds follows similar lines of analysis, though it is not reported here for the sake of conciseness.

We then exploited the magnifying lenses of the energy analysis to get some additional chemical clues on the redox potentials ranking within the set of the investigated compounds. Enthalpies of solvated systems and their changes upon reduction, may conveniently be decomposed in terms of atomic or atomic group contributions, using a Bader's partitioning of the molecular space and energies [27,29,30]. Energy analysis insights are then reflected in the spin density populations and in the thereof derived most important resonance structures for the reduced forms of the parents compounds (Figure 3).

We first identified a rationale for the redox potential ranking of the parent compounds (Table 2). The most and the least stable isomers in both initial and reduced forms are 1,2 and 1,4, respectively (see Table S1), but the latter compound has the highest redox potential because of its largest relative stabilization in the reduced form. The oxygen atoms are destabilized upon reduction in all systems (Table 2), despite they are increasing their negative net atomic charge by 0.05-0.08 electron (Figure 3). Since all O atoms experience similar changes in their atomic charges, their different energy destabilizations seem to be dominated by and related to the differences in their acquired electron spin polarization. The 1,2 compound has the smallest spin population on O atoms (0.13 electron and exclusively on O_2, Figure 3) and exhibits the lowest O destabilization (0.074 Ha) upon reduction. However, placing all the residual electron spin population on the remaining atoms, essentially the C atoms of the rings and in particular C_3, has a larger cost, so that this same compound has a significantly lower stabilization of the two five-membered rings (5MRs) upon reduction. It amounts to -0.212 Ha, compared to a value ranging between -0.265 and -0.288 Ha for the three other systems (Table 2). Energy stabilization upon reduction and the ensuing redox potential are therefore the result of a balance between O atoms destabilization and 5MR stabilization. Placing significant spin density on both O atoms – this may take place only in the two symmetric systems 1,6 and 1,4 (see Figure 3) - leads to large 5MR stabilization and higher potentials (2.78 and 2.82 V vs. Li^+/Li), despite the large oxygen atoms destabilization. Having large spin density on only one O atom, like in 1,5 and 1,2 compounds, results instead in smaller 5MR stabilization and lower redox potentials, 2.17 and 2.37 V vs. Li^+/Li, respectively (Table 2). The lowest potential value occurs for the 1,5 compound because of its twice as large overall spin population on O_5 compared with that on O_2 in 1,2. In fact, the ensuing larger O destabilization in the 1,5 compound is not entirely compensated for by its larger 5MRs stabilization and a lower potential comes up relative to the 1,2 system.

Reduction potentials for the N-substituted compounds may be likewise investigated (Table 3) by using the energy analysis of their parent compounds as a convenient reference. In fact, upon reduction, the relative weights of rings stabilization and O atoms destabilization roughly follow those of the corresponding parent compound. In general, the effect of N-substitution corresponds to a slight enhancement of the energy stabilization in the rings and to a moderate decrease in the O atoms destabilization upon reduction, thereby generating an augmentation in the reduction potential, relative to the parent compound. Ring energies in Table 3 include those of the N atoms that, similarly to the O atoms, become always destabilized upon reduction. However, differently from the case of O atoms, N atomic energies do not seem to follow analogous and clear trends with the N spin density populations. This is because the N atoms experience quite different electron population changes upon reduction,

Table 3, Parent compounds and their singly N-substituted pentalenedione derivatives: Reduction potentials (V) (in V *vs.* Li^+/Li), corresponding changes in subsystem energies from reduced to initial forms for ring 1 (R1) plus ring 2 (R2) (ΔE(R1+R2)), changes for global energy of oxygen atoms ($\Delta E(O_1+O_x)$) or nitrogen atoms (ΔE(N)) as well as total energy modification of the whole molecule (ΔE_{TOT}), variation of net atomic charges for Nitrogen upon reduction (Δq(N)), spin density population values (*S*) on O_1/O_x or O_1+O_x and N atoms in the reduced forms, *i.e.* $S(O_1)$, $S(O_x)$, $S(O_1+O_x)$ and *S*(N), respectively.

System	Voltage, V	ΔE(R1+R2)[a]	$\Delta E(O_1+O_x)$[a,b]	ΔE(N)[a]	ΔE_{TOT}[a]	Δq(N)	$S(O_1)$	$S(O_x)$[b]	$S(O_1+O_x)$[b]	*S*(N)
1,5_N (0,0)	2.173	-0.265	0.133	-	-0.132	-	0.014	0.251	0.265	-
1,5_N (3)	2.473	-0.279	0.137	0.011	-0.142	-0.054	0.094	0.219	0.313	0.056
1,5_N (4)	2.482	-0.253	0.111	0.071	-0.141	-0.059	-0.001	0.225	0.224	0.041
1,5_N (6)	2.531	-0.270	0.126	0.092	-0.144	-0.060	0.087	0.199	0.286	0.154
1,5_N (2)	2.625	-0.273	0.126	0.065	-0.148	-0.034	-0.013	0.262	0.249	0.187
1,2_N (0,0)	2.366	-0.212	0.074	-	-0.138	-	0.000	0.130	0.130	-
1,2_N (4)	2.695	-0.215	0.066	0.057	-0.149	-0.062	0.021	0.109	0.130	0.047
1,2_N (5)	2.791	-0.231	0.076	0.046	-0.155	-0.071	-0.012	0.165	0.153	0.118
1,2_N (6)	2.803	-0.221	0.067	0.030	-0.154	-0.096	0.025	0.116	0.141	0.073
1,2_N (3)	2.858	-0.221	0.065	0.088	-0.155	-0.034	0.013	0.062	0.075	0.264
1,6_N (0,0)	2.782	-0.272	0.119	-	-0.153	-	0.116	0.116	0.232	-
1,6_N (2)	3.066	-0.280	0.116	0.059	-0.164	-0.047	0.153	0.159	0.312	0.130
1,6_N (3)	3.089	-0.274	0.110	0.017	-0.165	-0.090	0.142	0.073	0.215	-0.029
1,4_N (0,0)	2.819	-0.288	0.134	-	-0.155	-	0.197	0.197	0.394	-
1,4_N (2)	3.118	-0.286	0.120	0.068	-0.166	-0.047	0.191	0.164	0.354	-0.002
1,4_N (3)	3.128	-0.297	0.131	0.018	-0.167	-0.084	0.233	0.154	0.387	-0.000

a) All energies are in Hartree (Ha). *b*) O_x is the second oxygen other than O_1.

depending on their location in the rings and on the carbonyl O position. Electron population changes, being not constant upon reduction as it roughly occurs for oxygen atoms, also play an important role in defining the N energy changes. It seems reasonable to suppose that N atoms are destabilized by their acquired spin population and stabilized by their increased electron population, the final N energy changes being related to the relative weight of these two factors, hence to the magnitudes and energy effectiveness of the electron and electron spin population changes (see Table 3).

It is worth noting that the highest potential within each N-substituted series of compounds (corresponding to the largest energy stabilization upon reduction) follows an interesting trend. Such a potential highlights the compounds having the largest spin density on N and the smallest increase of the electron population on N, *i.e.* those systems having asymmetrical carbonyl groups (1,2 and 1,5), the opposite being true for those with symmetrically placed carbonyls (1,4 and 1,6). In the highest potential derivatives of the latter, the N atoms replace C atoms bearing negligible – or even negative for the 1,6 system – spin densities in the parent compounds.

Finally, we examined the energy terms for those N-doubly substituted compounds (Table S3) that were found not to obey the energy additivity rule (Table 1). The derivatives [1,2_N(4,5)] and [1,4_N(2,3)] that exhibit an enhanced stabilization upon reduction relative to such rule have a largely enhanced ring stabilization and decreased O destabilization compared with the averages of the composing singly substituted systems, while the former effect is significantly dampened in the case of the [1,2_N(5,6)] compound, having an opposite deviation from the rule. In particular, upon reduction, the N atoms become more stable for the [1,2_N(4,5)] and [1,4_N(2,3)] systems, while they are largely destabilized in the reduced [1,2_N(5,6)] compound, analogously to what was noticed for the singly substituted derivatives. The anomalous behaviour for the former compounds may be likely ascribed to the conversion of an unfavourable N=N double bond to a more favourable N-N single bond, on passing from the initial to the corresponding reduced forms, see table S2. Favourable/unfavourable is here referred to only to the N stability. Note that having two contiguous N in a structure implies a large decrease of their electron population, relative to the case where they are separated. Typical differences are of the order of 0.4 e^- or more and are due to the fact the N turns out to be linked to only one and not to two electropositive C atoms (Table S4). When two contiguous N are linked through a double bond, such an N population decrease is further increased. It amounts to 0.8 e^- or even more, because the N is no longer able to withdraw the largest part of the π-electron pair as it does when the double bond lies between N and C. Data in Table S3 indeed show that in the [1,2_N(4,5)] and [1,4_N(2,3)] systems the two N globally increase their electron population by 0.6 and 0.42 e^- upon reduction, while in the [1,2_N(5,6)] compound the N-N bond distance decreases rather than increasing and the two N atoms even diminish their global population by 0.07 e^-.

Conclusions

We have described an unconventional theoretical approach to highlight the joined effects of isomerism and N single/double substitution in pentalenediones derivatives on voltages (*vs.* Li^+/Li). Such combined modification of the parent backbone was found to be very effective, leading to a global tuning as large as 2.2–3.6 V *vs.* Li^+/Li. While voltages range is limited to 2.2–2.8 V *vs.* Li^+/Li through the sole effect of isomerism, redox properties are largely improved by double N substitution for C. The value for the redox potential of the unsubstituted compound exerts a clear influence since single/double N substituted derivatives are shifted with respect to this initial starting point. One of the major clues of this work is the generally almost additive rule characterizing the double N substitution based on the combined actions of the composing single N substitutions and the identification of the chemical features causing the few exceptions to such rule. The success of our approach points to its potential and generality in tailoring the structure in view of engineering the redox activity of molecules and so promoting the discovery of new and advanced redox-active materials.

Acknowledgements

This work was financially supported by the Région Picardie and by the French National Research Agency (ANR). The research project used the computational resources from the GENCI-IDRIS, CCIPL (Centre de Calcul Intensif des Pays de Loire) and the computer centre MCIA of the University of Bordeaux and Pays de l'Adour.

Notes and references

1 X. Han, C. Chang, L. Yuan, T. Sun, J. Sun, *J. Adv. Mat.,* 2007, **19**, (12), 1616–1621.
2 H. Chen, M. Armand, G. Demailly, F. Dolhem, P. Poizot, J. -M. Tarascon, *ChemSusChem,* 2008, **1**, 4, 348–355.
3 W. Walker, S. Grugeon, O. Mentre, S. Laruelle, J. -M Tarascon, F. J. Wudl, *Am. Chem. Soc.,* 2010, **132**, 6517–6523.
4 M. Yao, H. Senoh, T. Sakai, T. Kiyobayashi, *Int. J. Electrochem. Sci.,* 2011, **6**, 2905–2911.
5 A.L. Barrès, J. Geng, G. Bonnard, S. Renault, S. Gottis, O. Mentré, C. Frayret, F. Dolhem, P. Poizot, *Chem. Eur. J.,* 2012, **18**, 8800–8812.
6 Z. Song, T. Xu, M. L. Gordin, Y. -B Jiang, I. -T Bae, Q Xiao, H. Zhan, J. Liu, D. Wang, *Nano Lett.,* 2012, **12**, 2205–2211.
7 G. Bonnard, A. -L Barrès, Y. Danten, D. G. Allis, O. Mentré, D. Tomerini, C. Gatti, E.I. Izgorodina, P. Poizot, C. Frayret, *RSC Advances,* 2013, **3**, 19081–19096.
8 Y. Liang, P. Zhang, J. Chen, *Chem. Sci.,* 2013, **4**, 1330–1337.
9 M. Yao, K. Kuratani, T. Kojima, T. Takeichi, H. Senoh, T. Kiyobayashi, *Sci Rep.,* 2014, **4**, 3650.
10 M. Armand, S. Grugeon, H. Vezin, S. Laruelle, P. Ribière, P. Poizot, J.-M Tarascon, *Nat. Mater.*, 2009, **8**, 120–125.
11 L. Fédèle, F. Sauvage, M. Becuwe, *J. Mater. Chem. A,* 2014, **2** (43), 18225–18228.
12 L. Fédèle, F. Sauvage, J. Bois, J.-M. Tarascon, M. Becuwe, *J. Electrochem. Soc.,* 2014, **161** (1), A46–A52.

13 V. A. Mihali, S. Renault, L. Nyholm, D. Brandell, *RSC Adv.,* 2014, **4**, 38004–38011.
14 S. W. Wang, L. J. Wang, Z. Q. Zhu, Z. Hu, Q. Zhao, J. Chen, *Angew. Chem. Int. Ed.,* 2014, **53**, 5892–5896.
15 E. Castillo-Martinez, J. Carretero-Gonzalez, M. Armand, *Angew. Chem. Int. Ed.,* 2014, **53**, 5341–5345.
16 S. Gottis, A. -L. Barrès, F. Dolhem, P. Poizot, *ACS Appl. Mater. Interfaces,* 2014, **6**, 10870−10876.
17 A. Shimizu, Y. Tsujii, H. Kuramoto, T. Nokami, Y. Inatomi, H. Nobuhiko, J.-i. Yoshida, *Energy Technology,* 2014, **2**, (2) 155–158.
18 A. Beheshti, P. Norouzi, M.R. Ganjali, *Int. J. Electrochem. Sci.,* 2012, **7**, 4811–4821.
19 M. Yao, H. Senoh, M. Araki, T. Sakai, K. Yasuda, *K. ECS Transactions,* 2010, **28** (8), 3–10.
20 D. Tomerini, C. Gatti, C. Frayret, *Phys. Chem. Chem. Phys.,* 2015, **17**, 8604–8608.
21 Gaussian 09, Revision D.01 M. J. Frisch, G. W. Trucks, H. B. Schlegel, G. E. Scuseria, M. A. Robb, J. R. Cheeseman, G. Scalmani, V. Barone, B. Mennucci, G. A. Petersson, H. Nakatsuji, M. Caricato, X. Li, H. P. Hratchian, A. F. Izmaylov, J. Bloino, G. Zheng, J. L. Sonnenberg, M. Hada, M. Ehara, K. Toyota, R. Fukuda, J. Hasegawa, M. Ishida, T. Nakajima, Y. Honda, O. Kitao, H. Nakai, T. Vreven, J. A. Montgomery, Jr., J. E. Peralta, F. Ogliaro, M. Bearpark, J. J. Heyd, E. Brothers, K. N. Kudin, V. N. Staroverov, R. Kobayashi, J. Normand, K. Raghavachari, A. Rendell, J. C. Burant, S. S. Iyengar, J. Tomasi, M. Cossi, N. Rega, J. M. Millam, M. Klene, J. E. Knox, J. B. Cross, V. Bakken, C. Adamo, J. Jaramillo, R. Gomperts, R. E. Stratmann, O. Yazyev, A. J. Austin, R. Cammi, C. Pomelli, J. W. Ochterski, R. L. Martin, K. Morokuma, V. G. Zakrzewski, G. A. Voth, P. Salvador, J. J. Dannenberg, S. Dapprich, A. D. Daniels, O. Farkas, J. B. Foresman, J. V. Ortiz, J. Cioslowski and D. J. Fox, Gaussian, Inc., Wallingford CT, 2009.
22 A.V. Marenich, C.J. Cramer, D.G. Truhlar, *J. Phys. Chem. B,* 2009, **113**, 6378–6396.
23 J. Guerard, J. S. Arey, *J. Chem. Theory Comput.*, 2013, **9**, 5046−5058.
24 J. E. Bachman, L. A. Curtiss, R. S. Assary, *J. Phys. Chem. A*, 2014, **118**, 8852−8860.
25 S.D. Pineda Flores, G.-C. Martin-Noble, R.L. Phillips, J. Schrier, *J. Phys. Chem. C,* 2015, **119**, 21800-21809.
26 J. M. Vollmer, L. A. Curtiss, D. R. Vissers, K. Amine, *J. Electrochem. Soc*. 2004, **151**, A178.
27 R. F. W. Bader, *Atoms in Molecules: A Quantum Theory*, Clarendon Press, Oxford, 1994.
28 C. Gatti, SF-ESI codes, private communication.
29 A. A. Arabi, C. F. Matta, *J. Phys. Chem. A,* 2009, **113**, 3360–3368.
30 C. F. Matta, N. Castillo, R. J. J. Boyd, *Chem. Phys.,* 2006, **125**, 204103.